$$\times \frac{[N(-\omega_2/k_2) - N(\omega_1/k_1 - \omega_n/k_n)] \cdots \{N(-\omega_{n-1}/k_{n-1}) - N[\sum_{l=1}^{n-2} (\omega_l/k_l - \omega_n/k_n)]\}}{k_n\omega_n - k_{n-1}\omega_{n-1} \cdots k_1\omega_1}, \tag{A6}$$

and the contribution to the Helmholtz free energy is equal to

$$-\frac{1}{\beta}\frac{(-\beta)^2}{2!} n! \sum_{\lambda_1 \cdots \lambda_n} |V(\lambda_1, \lambda_2, \ldots, \lambda_n)|^2$$

$$\times \sum_{n_1, n_2, \ldots, n_{n-1}} G(\lambda_1, i\omega_{n_1}) G(\lambda_2, i\omega_{n_2}) \cdots G(\lambda_{n-1}, i\omega_{n-1}) G(\lambda_n, -i\omega_{n_1} - i\omega_{n_2} \cdots - i\omega_{n_{n-1}})$$

$$= -\frac{1}{\hbar}\frac{n!}{2!} \sum_{\lambda_1 \cdots \lambda_n} |V(\lambda_1, \lambda_2, \ldots, \lambda_n)|^2 \times \text{Eq. (A6)}. \tag{A7}$$

*Work supported by the National Research Council of Canada.

[1]L. Van Hove, *Quantum Theory of Many Particle Systems* (Benjamin, New York, 1961).
[2]A. A. Maradudin, P. A. Flinn, and R. A. Coldwell-Horsfall, Ann. Phys. (N. Y.) 15, 360 (1961).
[3]C. R. Brooks, J. Phys. Chem. Solids 29, 1377 (1968); A. J. Leadbetter, D. M. T. Newsham, and G. R. Settatree, J. Phys. C 2, 393 (1969).
[4]P. F. Choquard, *The Anharmonic Crystal* (Benjamin, New York, 1967).
[5]V. V. Goldman, G. K. Horton, and M. L. Klein, Phys. Rev. Letters 21, 1527 (1968).
[6]M. Born and K. Huang, *The Dynamical Theory of Crystal Lattices* (Clarendon, Oxford, England, 1954).
[7]R. A. Cowley, Advan. Phys. 12, 421 (1963).
[8]W. Ludwig, J. Phys. Chem. Solids 4, 283 (1958).
[9]J. W. Leech and J. A. Reissland, J. Phys. C 3, 975 (1970); 3, 987 (1970).
[10]M. L. Klein, V. V. Goldman, and G. K. Horton, J. Phys. C 2, 1542 (1969).
[11]M. L. Klein, G. K. Horton, and J. L. Feldman, Phys. Rev. 184, 968 (1969).

PHYSICAL REVIEW B VOLUME 3, NUMBER 12 15 JUNE 1971

Superconductivity and Lattice Dynamics of White Tin

J. M. Rowell, W. L. McMillan, and W. L. Feldmann
Bell Telephone Laboratories, Murray Hill, New Jersey 07974
(Received 6 January 1971)

We present the results of a tunneling investigation and the details of the electron-phonon interaction in superconducting tin. From an iterative solution of the Eliashberg gap equations, the phonon spectrum, weighted by the square of the electron-phonon coupling constant, is determined. Comparison of this result with neutron scattering data suggests that, as in Pb, off-symmetry directions must be considered carefully in any determination of the tin phonon spectrum. The resolution and reproducibility of the tunneling technique is discussed at some length; in particular, we show that the Coulomb pseudopotential μ^* is extremely sensitive to small experimental errors. We suggest that a value of μ^* near the theoretical value of 0.10 can be taken as an indication of acceptably accurate experimental measurements.

I. INTRODUCTION

During the past six years a new technique for the study of both superconductivity and lattice dynamics has been developed. This technique, using electron tunneling into a superconductor, allows us to probe the details of the electron-phonon interaction that determines the superconductivity of the material. In this paper we present the results of such an investigation of the properties of white tin. The phonon spectrum, weighted by the square of the electron-phonon coupling constant, is determined. Comparison of this result with neutron scattering data suggests that, as in Pb, off-symmetry directions must be considered carefully in any determination of the tin phonon spectrum.

The first measurement of a superconducting property using the tunneling technique was made by Giaever[1] when he demonstrated the existence of the energy gap and, above the energy gap, the

square-root singularity in the electronic density of states of Pb. Later measurements by Giaever *et al.*[2] confirmed the close agreement between the normalized conductance of the tunnel junction and the quasiparticle density of states predicted by Bardeen, Cooper, and Schrieffer (BCS).[3] In the case of Pb, however, deviations from the expected density of states were observed[2] over the energy range $2\Delta_0$ to $k\Theta_D$, where Δ_0 is the energy gap and Θ_D the Debye temperature. These were interpreted in terms of a gap parameter which was made energy dependent by details of the electron-phonon interaction, as demonstrated earlier by Swihart[4] for simple phonon distributions. A calculation of the density of states by Culler *et al.*,[5] based on a Debye model for the spectrum of the phonons involved in the electron-electron interaction, was unable to reproduce the double structure in the conductance observed by Giaever *et al.* However, more detailed measurements of this conductance and particularly its derivative (d^2I/dV^2) indicated[6] that a more realistic model of the phonon spectrum was necessary. Schrieffer *et al.*[7] pointed out that the expression for the tunneling density of states had to be modified for a complex gap parameter. Using a model phonon spectrum of Lorentzian peaks in the transverse and longitudinal regions, they calculated a density of states which was in encouraging agreement with the experimental result. This approach to the problem of understanding the superconducting properties of a material, namely, to first find the essential normal-state parameters from independent experiments or from calculation, has been extended recently by Dynes *et al.*,[8] who used more accurate phonon spectra. They calculated $\alpha^2(\omega)F(\omega)$, including the critical points in $F(\omega)$, from neutron scattering results. Hence, by a single solution of the gap equation, they found the density of states $N(\omega)$ and its derivative to compare with experimental tunneling derivatives.

We developed[9,10] an alternative, more direct, approach to the problem of determining the gap parameter $\Delta(\omega)$, the phonon spectrum $F(\omega)$ weighted by the electron-phonon coupling parameter $\alpha^2(\omega)$, and the Coulomb pseudopotential μ^*. This is to take the experimental tunneling result for $N(\omega)$ and derive, by an iterative procedure, the normal-state parameters which, when used in a solution of the gap equation, give derivatives of the tunneling characteristic in exact agreement with experiment. This method has been described in some detail previously[10] and applied to Pb most extensively. The theory of the strongly coupled superconductor has been reviewed by Scalapino[11] in the same book. In view of these two articles, we feel that it is unnecessary to present the theory or the technique at length again. However, measurements on tin, which is not generally considered a strongly coupled material, present somewhat more of an experimental challenge than Pb, as the deviations from BCS behavior are five times weaker for Sn. We report in this paper such a study of Sn which allows us to estimate the accuracy (and reproducibility) of the derivative measurements and the resulting errors in $\alpha^2(\omega)F(\omega)$. In particular, we find there is a very simple way to judge the validity of the derivative data and the significance of the calculated $\alpha^2(\omega)F(\omega)$. This is simply to check that the value of μ^* obtained from the experiment falls within the range 0.09–0.14. As we will show, this parameter is remarkably sensitive to errors in the determination of the derivatives and the energy gap.

II. EXPERIMENTAL

A. Sample Preparation

The tunnel junctions used in the investigation of tin were of two types: tin–tin oxide–tin (Sn-*I*-Sn) and aluminum–aluminum oxide–tin (Al-*I*-Sn). These were prepared in the conventional thin-film form by evaporation in an oil-pumped vacuum system at pressures $\sim 10^{-6}$ Torr. The junction arrangement has been shown previously.[12] In the Sn-*I*-Sn case the junction areas were $\sim 2\times10^{-4}$ cm^2; for Al-*I*-Sn this was increased to $\sim 5\times10^{-3}$ cm^2 to obtain junction resistances in the desired range (20–100 Ω). The oxidation of aluminum was accomplished by exposing the freshly evaporated film to air from the laboratory for about 1 min. The oxidation of tin is a little more difficult and two approaches have been used. The earlier junctions were prepared by thermal oxidation, usually by heating the tin to ~ 100 °C in air for a few hours. On occasion, damp air or oxygen was used; as the success of this technique seems to vary from one laboratory to the next it is misleading to be more specific. The thermal oxidation of tin, and even more so lead, appears to be a matter for individual trial and error. A more reliable technique appears to be "glow discharge oxidation"[13] and this was used for the recent Sn-*I*-Sn junctions. In our case, the glass substrate, with its first tin film, was removed from the evaporator and placed in a small bell jar which was then evacuated using a rotary pump only. The bell jar had an aluminum base plate (anode, grounded) and aluminum cathode inserted through the glass. Using a leak valve a pressure of 50 μ of oxygen was obtained and a discharge at 700 V maintained ~ 2 min. The tin film was shielded from the cathode by a glass plate. The small system was then vented with oxygen and the sample again transferred to the evaporator. This oxidation has been consistently successful and is more reliable than thermal oxidation.

The tin films, ~ 2000 Å thick, were evaporated from tungsten conical baskets or molybdenum boats

onto glass substrates at room temperature. The evaporation rate was great enough to produce shiny films, as opposed to the gray surfaces which result from a slow evaporation onto warmer substrates. We have recently used only bulk tin and lead for evaporations. Material in wire form, although allegedly 99.999% pure, gave distinctly poorer tunneling characteristics which will be discussed below. The completed junctions, with electrical contacts of fine gold wire attached with indium solder or silver paste, were immersed directly into liquid nitrogen and then into liquid helium. Subsequently, they were not cycled to room temperature, if necessary being stored in liquid nitrogen until measurements were complete.

B. Junction Evaluation

With the junctions at ~1 K, an examination of the I-V characteristics alone is generally sufficient to determine whether further measurements are worthwhile. The criteria used are (a) that the resistances of the five junctions should scale with their area to ±20%; (b) the superconducting conductance at $V=0$ should be $\sim 10^{-3}$ of the normal-state conductance; (c) the negative resistance region $\Delta_{Sn} - \Delta_{Al} < V < \Delta_{Sn} + \Delta_{Al}$ should be well defined in Al-I-Sn junctions; (d) there should be only small currents flowing for $\Delta < V < 2\Delta$ in Sn-I-Sn junctions; (e) the "zero-bias anomaly" in the normal state should be small. The first two of these checks have been discussed before[10] but the importance of the other three has been realized more recently and some elaboration may be justified. We have found that in some Al-I-Sn junctions, although condition (b) above may be met, an appreciable current may flow just below $\Delta_{Sn}-\Delta_{Al}$ and appears to increase with voltage. This results in a smearing of the negative-resistance region. The reason for this behavior in Al-I-Sn is not known, but in the case of Al-I-Pb such "poor" characteristics always resulted from evaporating Pb which was supplied as wire, although the purity was claimed to be 99.999%. Good characteristics were obtained from the evaporation of bulk Pb (also 99.999%) under similar conditions. The contaminant in the wire (introduced by the drawing process?) has not yet been identified. The junctions with poor characteristics consistently showed a reduction in the strength of the strong-coupling density-of-states structure of 5 to 10%. This reduction was sufficient to affect the results of the gap inversion program.

The problem of the normal-state zero-bias anomaly[14] is only encountered in our Sn-I-Sn junctions, as it does not occur in our aluminum-oxide or lead-oxide barriers. This zero-bias conductance peak is explained[15] in terms of scattering by localized magnetic impurities in the tin oxide. The magnitude of the peak, which depends on the oxidation procedure and the past history of the evaporator used to make the films, varies from ~7% to <0.1% of the background conductance at $V=0$. One immediately suspects that the superconducting properties of the films would be affected by these magnetic impurities, although our results are inconclusive on this point. Experimentally, the main difficulty in using these junctions is that, as the magnitude of the anomaly increases, the conductance increases[14] more rapidly with voltage over the phonon range (0–20 meV). This rapidly rising conductance makes normalization of the first-derivative data more difficult. In practice, we used Sn-I-Sn junctions with 0.0–0.2% anomalies. The oxide produced in the glow discharge always had such small anomalies. It may be worth noting that superconducting tunneling data obtained on junctions showing "giant anomalies" are known to be in serious error in some cases. For example, in Cr-I-Pb junctions the gap characteristics is well resolved but the phonon-induced structure is about one-fifth of its correct size.[14] In "doped" Sn-I-Pb junctions, Shen reports[16] that the phonon–density-of-states structure of the Pb is unobservable. In Ta and Nb junctions, if the surface of the metal is not cleaned carefully,[17] the phonon structure is nonexistent, the gap characteristic is very poor, and the zero-bias conductance anomaly can be very strong.

C. Measurements

The essential parameters which must be determined experimentally are the energy gap Δ_0 and the normalized first derivative of the tunneling characteristic from just above Δ_0 to an energy greater than the maximum phonon frequency.

Although not essential, a determination of T_c for Sn is useful, as rather high transitions have been reported for films. The T_c for a Sn film made in the same way as those in the junctions was determined, using the method of Feldmann and Rowell,[18] to be 3.76 K. This is close to the bulk value of 3.72 K and the films in each junction were not investigated individually.

The energy gap Δ_0 was found by displaying the I-V characteristic at low voltages for both bias directions. Following the construction outlined before,[10] the sum of the midpoints of the rise in current was taken to measure $4\Delta_0$ in the Sn-I-Sn junctions. The gap values, given in Table I, range from 0.605 to 0.62 mV. These are measured at ~0.95 K; the change in gap on extrapolating to zero temperature is insignificant (≈ 1 in 10^3).

Conventional modulation techniques were used to measure the normalized first derivative.[10] As the deviations from the BCS density of states are so small, we used the ac bridge whose circuit is shown correctly in Fig. 1 of Ref. 19. The second derivative was also measured directly using the

TABLE I. Details of the junctions used in this investigation and their method of preparation. We also give the energy gap (Δ_0), the strength of the phonon induced deviations from a BCS density of states (N_{ph}), this strength normalized to Δ_0^2, three different averages over the phonon spectrum defined in the text ($\bar{E}$, A^2, and λ), the Coulomb pseudopotential μ^*, and three average phonon frequencies also given in the text ($\langle\omega\rangle$, $\bar{\omega}$, and $\langle\omega^2\rangle$).

Sample	Oxidation	Δ_0 (mV)	N_{ph}	N_{ph}/Δ_0^2	$\bar{E}$ (meV^2)	A^2 (meV)	λ	$\langle\omega\rangle$ (meV)	μ^*	$\bar{\omega}$ (meV)	$\langle\omega^2\rangle$ (meV^2)
Sn-*I*-Sn 92867	Thermal	0.62	0.0139	0.0362	38.9	3.48	0.77	9.04	0.109	11.2	101
Sn-*I*-Sn 8967	Thermal	0.61	0.0134	0.0361	37.6	3.32	0.71	9.35	0.090	11.3	106
Sn-*I*-Sn 121868	Discharge	0.609	0.0131	0.0354	41.1	3.57	0.77	9.27	0.133	11.5	107
Sn-*I*-Sn 31469	Discharge	0.606	0.0131	0.0357	39.3	3.42	0.72	9.50	0.111	11.5	109
Al-*I*-Sn 41769	Thermal	0.605	0.0131	0.0358	43.1	3.74	0.80	9.35	0.145	11.5	108

circuit of Thomas and Rowell.[20]

The importance of measuring both the normal- and superconducting-state resistances with equal accuracy is demonstrated very clearly in Fig. 1, where we show the derivatives for an AlMn-*I*-Sn junction at 0.35 K. (The AlMn alloy contained a few percent of manganese before evaporation, but this was not sufficient to give an entirely normal film at 0.35 K.) It can be seen that the normal-state resistance is very asymmetrical about zero bias and also exhibits structure over this energy range. It is believed that the asymmetry is primarily determined by details of the tunneling barrier,[21] and that the structure is due to excitation of phonons of the electrodes by the tunneling electrons.[10,19,22] We also include in Fig. 1 the measured superconducting-state second derivatives for the two bias directions, illustrating again that the asymmetry of the normal resistance cannot be ignored, even in second derivatives. It is also apparent that the Sn positive bias is the preferred direction, both for ease of normalization of the first derivatives and for resolution of fine structure in the second derivative. Even more detailed second derivatives are obtained for Sn-*I*-Sn junctions without going to such low temperatures (see, for example, Fig. 12 of Ref. 12). Despite the asymmetries of Fig. 1, the only parameter whose magnitude is important is the normalized first derivative, which was determined for both biases and found to agree within a few parts in 10^4. This means the strength of the phonon-induced structure is identical to within a few percent, which, as will be shown below, appears to be the reproducibility of our measurements.

A further problem arising from results such as those shown in Fig. 1 is the question of what changes in the phonon-emission structure occur when the Sn becomes superconducting. For example, an electrode phonon of energy ω_{ph} will give rise to a step increase in conductance at a voltage given by $V=\omega_{ph}/e$ in the normal state, but in the superconducting state the increase will reflect the square-root singularity in the density of states above the gap and will occur at a voltage $V=(\omega_{ph}+\Delta_{Al}+\Delta_{Sn})/e$. At one time we included[10] a correction for this effect by determining the "barrier and electrode phonon density" (the derivative of the even conductance), folding this with the appropriate gap singularities and shifting in voltage by $\Delta_{Al}+\Delta_{Sn}$. This then gave a corrected "normal conductance" which included the changes which would result from making the electrodes superconducting. However, we decided that the resulting corrections to the normalized density of states were no larger than the reproducibility of our measurements between different junctions.

D. Data Reduction

The first stage of calculation is simply to reduce the dynamic resistances in the superconducting and normal states (R_S and R_N), which are obtained as punched-paper-tape output, to the normalized conductance G_s/G_n (where G_s is the superconducting-state conductance and G_n is the normal-state con-

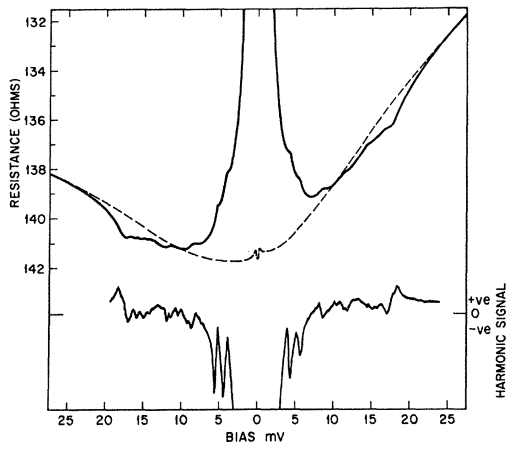

FIG. 1. Dynamic resistance dV/dI of an AlMn-*I*-Sn junction at 0.35 K in both the normal and superconducting states. The most rapid change in resistance occurs for the Al positive bias. The lower part of the figure shows the harmonic signal (roughly d^2I/dV^2) for the same junction.

ductance). Incorporation of the second-derivative data assures that a point-to-point differentiation of this normalized first derivative will reproduce all the fine structure which is resolved most easily in d^2I/dV^2. The magnitude of structure in this normalized first derivative, however, is determined solely from G_s/G_n.

From the normalized conductance, the density of states of Sn is found in the second stage of calculation. (The programs we used in all three stages have been distributed rather widely and copies are available as a technical report.[23]) In the case of Sn-*I*-Sn junctions the density of states is assumed to be the same in each film, in Al-*I*-Sn junctions the aluminum film is taken to have a BCS density of states derived for the measured energy gap of Al. Any phonon effects in Al are at least 20 times weaker than those in Sn, so the BCS density is a good approximation. Zero temperature is assumed throughout.

The resulting density of states $N(\omega)$ is shown in Fig. 2, where it is compared with the density for a BCS superconductor $[N(\omega)_{BCS}]$ with the same energy gap. In order to display the phonon effects (i.e., deviations from the BCS dependence) more clearly, and to avoid the rapid rise in density at low energies, we compute $N(\omega)/N(\omega)_{BCS}$, which is shown in Fig. 3. This is a convenient point to determine the reproducibility of our data as, in order to obtain the plot of Fig. 3, we have used three derivative measurements (R_S, R_N, d^2I/dV^2) and our measurement of the tin gap Δ_0 (also Δ_0 for aluminum in Al-*I*-Sn junctions). Thus, all the errors in the four essential measurements will be reflected in Fig. 3. Rather than attempt to superimpose the results for a number of different junctions, we have shown the plot derived from Fig. 2 and at selected energies have shown the magnitudes obtained for

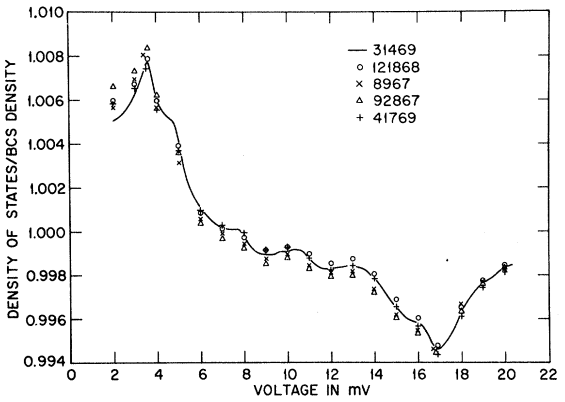

FIG. 3. Superconducting density of states in tin divided by the BCS density of states for a superconductor with the same gap. The solid line is for one particular junction; the symbols give the value of this ratio of densities at selected voltages for four other junctions. The voltage is measured from Δ_0.

four other junctions. Details of the junctions are given in Table I. The fine structure in the solid line is reproduced in detail in each junction, and the experimental resolution for any one junction is considerably better than 1 in 10^4, however, the reproducibility of the data is approximately ± 0.0004. As the total strength of the phonon effects is 0.0135, this is a total uncertainty of 6%. More consistent data can be obtained for Pb as the phonon effects are about five times stronger.[10] A large part of the variations between tin junctions is apparently due to small differences in the gap of the films (and presumably in T_c). This can be seen in Table I where we have given the total strength of the phonon effects N_{ph} as the sum of the maximum deviations from $N(\omega)_{BCS}$ which occur at 3.6 and 17 mV, respectively. It is seen that this

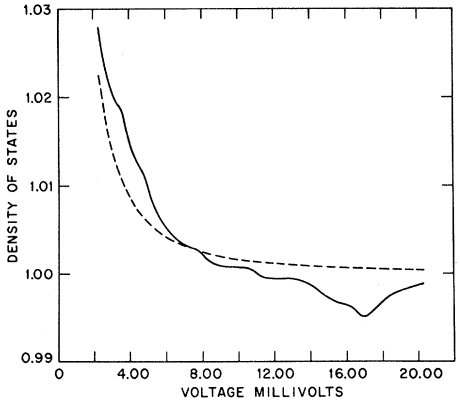

FIG. 2. Superconducting density of states in tin, covering the voltage range from Δ_0 to above the maximum phonon frequency. The dashed line is the BCS density of states for a superconductor with the same gap Δ_0.

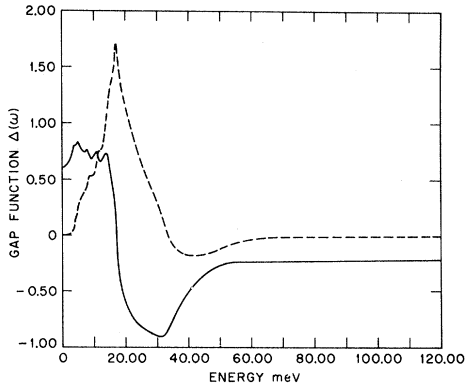

FIG. 4. Gap function $\Delta(\omega)$ vs energy in tin. The solid and dashed lines show the real and imaginary parts, respectively.

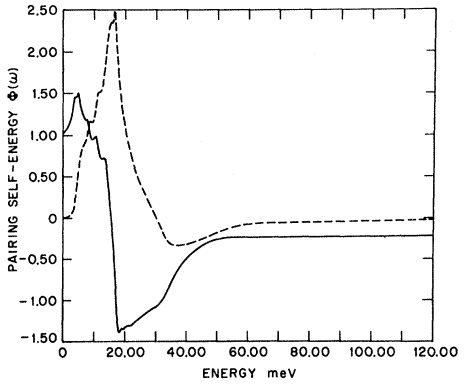

FIG. 5. Pairing self-energy $\phi(\omega)$ vs energy in tin. The solid and dashed lines show the real and imaginary parts, respectively.

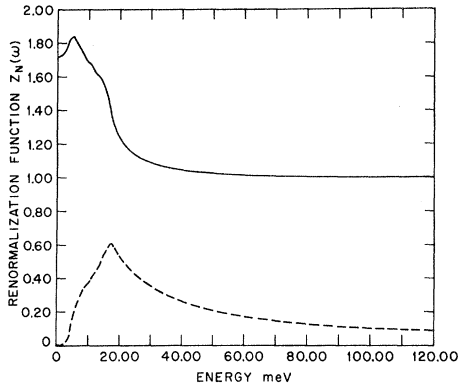

FIG. 7. Normal-state renormalization function $Z_N(\omega)$ vs energy in tin. The solid and dashed lines show the real and imaginary parts, respectively.

strength scales with the gap; in fact, it should be proportional to Δ_0^2. In Table I we give values for N_{ph}/Δ_0^2 and the total spread over the five junctions is only 2.5%. This represents the accumulated errors of our measurements.

The third stage of calculation, the iterative solution of the Eliashberg gap equation to obtain the normal-state parameters [μ^*, $\alpha^2(\omega)F(\omega)$, $\Delta(\omega)$, etc.], has been described for Pb and, as mentioned above, is available as a technical report.[23] The number of iterations required is determined by studying a plot of the experimental density of states divided by the density calculated from the derived parameters. For the junctions listed in Table I, a ratio of 1.0 within 1×10^{-4} to 3×10^{-4} is obtained, again being at most 2.5% of the strength of the phonon effects. Except at very low energies, the lack of fit is generally independent of energy, indicating a constant error in the normalization of the superconducting and normal derivatives. This is not unexpected, as the change from superconducting to normal states can cause a redistribution of current in the junction area.[24]

The sensitivity of the Coulomb term μ^* to the small errors in the data outlined above can also be seen in Table I, where its value ranges from 0.09 to 0.145. Because of this sensitivity, we do not believe that the tunneling technique can be used to determine an accurate μ^*, but rather take a result of 0.11 ± 0.03 as a confirmation of the theoretical value[25] of 0.10 and also as an indication of acceptably accurate input data. This value of μ^*, namely, 0.11 ± 0.03, can be used as a general check of experimental accuracy, as it has been shown by Morel and Anderson[25] that μ^* for most superconductors will fall within this range.

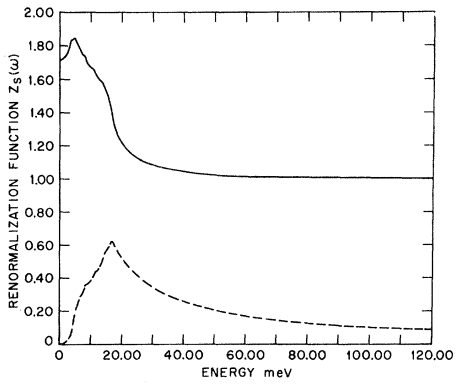

FIG. 6. Superconducting-state renormalization function $Z_s(\omega)$ vs energy in tin. The solid and dashed lines show the real and imaginary parts, respectively.

III. RESULTS AND DISCUSSION

The iterative solution of the gap equation yields both real and imaginary parts of the gap function $\Delta(\omega)$ and also the pairing self-energy $\phi(\omega)$ and renormalization function $Z_s(\omega)$ (both for $\omega > \Delta_0$) with $\Delta(\omega) = \phi(\omega)/Z_s(\omega)$. A further computation then gives the renormalization function for the normal state $Z_n(\omega)$. The four parameters are presented in Figs. 4–7 and represent a complete description of the dynamics of the electron-phonon interaction in tin. The plots exhibit detailed structure, due to multiphonon processes, up to roughly twice the maximum phonon frequency. As the determination of $N(\omega)$ is confined to the energy range shown in Fig. 3, this higher-energy structure is generated by the multiphonon emission terms of the gap equation itself. We have shown,[10] however, that for Pb the calculated $N(\omega)$ in this multiphonon region is in good agreement with a measurement extended into this region, thus confirming the accuracy of the gap equation.

The renormalization function $Z_N(\omega)$, shown in

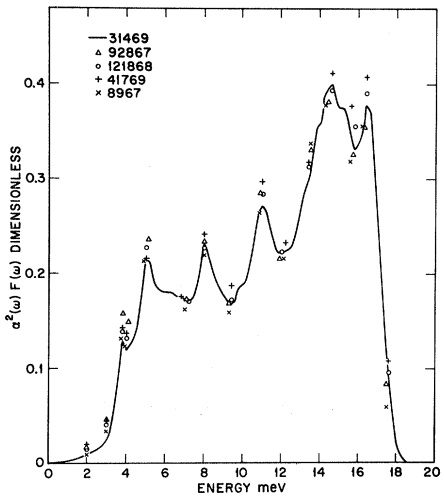

FIG. 8. Energy dependence of the tin phonon spectrum $F(\omega)$ weighted with the electron-phonon-coupling parameter $\alpha^2(\omega)$. The solid line was obtained by an iterative solution of the gap equations from the solid-line data in Fig. 3. At 2, 3, 13.4, or 13.5 meV and at 17.5 or 17.6 meV the value of $\alpha^2(\omega)F(\omega)$ is given for the four other junctions included in Fig. 3. At all other energies symbols are placed at a maximum or minimum in $\alpha^2)(\omega)F(\omega)$ and give the corresponding energy of this maximum or minimum.

Fig. 7, is useful information for experiments, such as the Tomasch effect,[26] which involve electrons with sufficient energy to emit phonons. The electron velocity measured by the Tomasch oscillations is $v_F/\mathrm{Re}Z_N(\omega)$, but for oscillations to be observed at all, the mean free path of the electrons

$$l_{\mathrm{ph}}=\hbar v_F/2\,\mathrm{Im}Z_N(\omega)$$

must be comparable to twice the thickness of the film.[27] The electron self-energy Σ is equal to $[Z_N(\omega)-1]\omega$.

The most interesting result obtained from the experiment is, of course, the product function $\alpha^2(\omega)F(\omega)$, which is shown in Fig. 8. The result is derived from data of Fig. 3 and we again show point values for other junctions. The low- and high-energy extremes of the spectrum are the most seriously affected by experimental errors, the low end because the rising density of states makes the measurement more difficult and errors in Δ_0 have their greatest effect, the high end because, for a given phonon density, the strength of the induced structure in conductance decreases as $1/\omega^2$. Again it should be stressed that all the detailed structure of the solid line of Fig. 8 is reproduced from junction to junction but the relative strength of the peaks and over-all shape of the spectrum vary enough to give the scatter indicated at each point. In view of the relatively slow energy dependence expected for $\alpha^2(\omega)$,[11,28] the plot of $\alpha^2(\omega)F(\omega)$ is essentially a measurement of $F(\omega)$, especially if one is interested in the fine structure of the spectrum rather than in over-all magnitudes. The third stage of calculation also gives three useful averages over the weighted phonon spectrum which may be defined as

$$\overline{E}=\int_0^\infty \omega\,\alpha^2(\omega)\,F(\omega)\,d\omega\ ,$$

$$A^2=\int_0^\infty \alpha^2(\omega)\,F(\omega)\,d\omega\ ,$$

and the dimensionless electron-phonon-interaction strength

$$\lambda=2\int_0^\infty \frac{\alpha^2(\omega)\,F(\omega)}{\omega}\,d\omega\ .$$

From these values, given in Table I, average phonon frequencies, used for example in recent T_c equations, can be defined as $\overline{\omega}=\overline{E}/A^2$, $\langle\omega\rangle=2A^2/\lambda$, and $\langle\omega^2\rangle=2\overline{E}/\lambda$. These values are also given for each junction in Table I. The lack of reproducibility in these parameters is somewhat disappointing but again illustrates their sensitivity to the exact shape of the phonon spectrum.

To our knowledge, tunneling is the only experimental technique which, to date, has determined a spectrum as detailed as that shown in Fig. 8. The lattice dynamics of tin has been the subject of numerous previous studies, both theoretical[29,30] and experimental,[31–37] the latter mostly using the more conventional technique of neutron scattering. Generally, the measurements have been limited to the symmetry directions of the crystal. The difficulty of extending such measurements to off-symmetry directions has recently been illustrated for Pb and is expected to be even more severe for Sn. In the case of Pb the neutron measurements[38] were extended[39] using the Born–von Karman model and it was apparent that the resulting $F(\omega)$ was only in moderate agreement with the $\alpha^2(\omega)F(\omega)$ tunneling result. For example, the transverse-phonon peaks differed in energy by 17%. It was pointed out by Dynes *et al.*[28] that the critical points in most obvious disagreement with the tunneling result were, in fact, generated by the Born–von Karman analysis in off-symmetry directions. More detailed neutron measurements by Stedman *et al.*,[40] who included many off-symmetry directions, confirmed that the earlier analysis led to these erroneous critical points. Their extensive measurements allowed them to construct a phonon spectrum without recourse to a model calculation. Their resulting $F(\omega)$ is in remarkably good agreement with $\alpha^2(\omega)\times F(\omega)$ from tunneling.[41] In view of these difficulties with Pb, the more complex lattice structure and

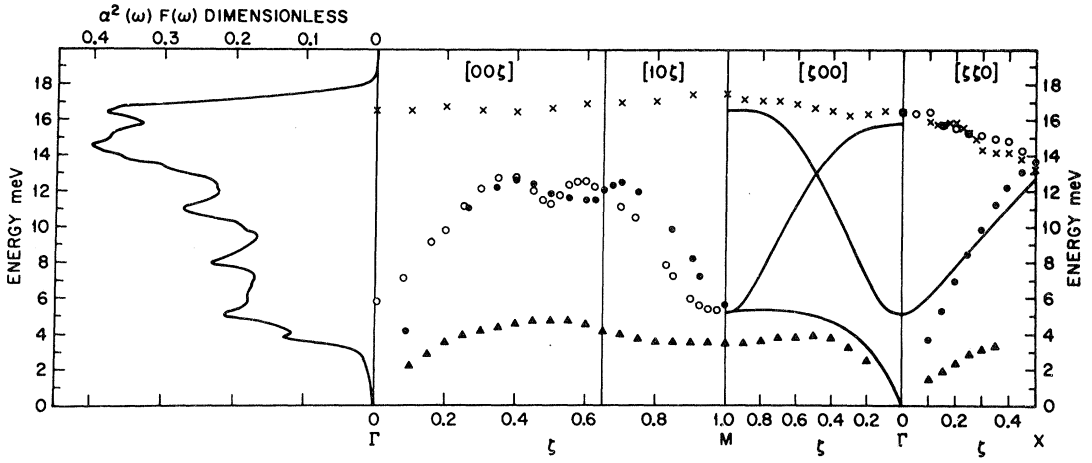

FIG. 9. Comparison of the tunneling result $\alpha^2(\omega)F(\omega)$ with the dispersion curves determined by neutron scattering. The neutron measurements shown by symbols are from J. M. Rowe (Ref. 36), being taken at 110 K. The solid lines are *room-temperature* measurements from Long Price (Ref. 35).

Fermi surface of tin suggests that a model calculation of the phonon spectrum, based only on symmetry direction measurements, will never be successful. This point has been stressed by Rowe, [36] who found that 20 parameters were required to fit only one branch of the dispersion curves.

Despite the lack of a phonon spectrum from the neutron data, we can compare $\alpha^2(\omega)\,F(\omega)$ with the dispersion curves themselves. We have done this in Fig. 9, where we have used Rowe's results taken at 110 K. More extensive data at room temperature have been reported by Long Price[35] and we have sketched in the extra branches he found. In the dispersion curves of Fig. 9, regions of high phonon density occur where the branches are relatively flat. The agreement at the high- and low-energy ends of the spectrum is good but in the intermediate energy range (6–13 meV) is less satisfactory. The tunneling peak at 11 meV falls lower than most of the 001 branch out to H, suggesting that the true critical points for this branch may occur away from this symmetry direction. More serious is the observation of a tunneling peak at 8 meV which has no obvious origin in the dispersion curves. From measurements made in off-symmetry directions, however, Long Price[42] has evidence that about midway between the 100 and 001 directions a critical point occurs at this energy because of a maximum in the lowest transverse branch, or crossing of the two lowest branches. In view of this interesting apparent discrepancy between the tunneling result and the dispersion curves, at least along the symmetry directions, further, more detailed, measurements of the dispersion curves away from the symmetry directions appear to be in order.

A second way of obtaining $F(\omega)$ is to measure the incoherent scattering of neutrons. For a few materials, such as vanadium, [43] this has given $F(\omega)$ directly. For materials which scatter coherently, an alternative approach is to use a polycrystalline target. This method has been used for Te, Pb, and Sn polycrystals by Kotov and co-workers, [37,44] and for Pb and $Pb_{40}Tl_{60}$ by Roy and Brockhouse, [45] whose targets were an assembly of pellets. Both results for Pb are in good agreement with the tunneling data while the spectrum for Sn obtained by Kotov *et al.* shows a strong over-all similarity to our result of Fig. 8. However, the neutron result appears to have more phonon strength in the 3- to 4-meV range; unfortunately, it is not possible to make any realistic comparisons of the positions of individual peaks in the two spectra.

We have demonstrated the ability of the tunneling technique to measure the weighted phonon spectrum $\alpha^2(\omega)\,F(\omega)$ of a material with a relatively complicated lattice structure. We obtain more detailed resolution of fine structure in the spectrum than any other technique which is currently available. The reproducibility, even for this relatively low-T_c material, is much better than that obtained between the spectra calculated using different models and the dispersion curves. A comparison of our result with the dispersion curves shows that a more detailed neutron scattering study of the off-symmetry directions would be worthwhile, as some peaks in $\alpha^2(\omega)\,F(\omega)$ are not obviously connected with the dispersion curves in the symmetry directions.

[1] I. Giaever, Phys. Rev. Letters 5, 147 (1960).
[2] I. Giaever, H. R. Hart, and K. Megerle, Phys. Rev. 126, 941 (1962).
[3] J. Bardeen, L. N. Cooper, and J. R. Schrieffer, Phys. Rev. 106, 162 (1957); 108, 1175 (1957).
[4] J. C. Swihart, IBM J. Res. Develop. 6, 14 (1962).

[5]G. J. Culler, B. D. Fried, R. W. Huff, and J. R. Schrieffer, Phys. Rev. Letters 8, 399 (1962).
[6]J. M. Rowell, P. W. Anderson, and D. E. Thomas, Phys. Rev. Letters 10, 334 (1963).
[7]J. R. Schrieffer, D. J. Scalapino, and J. W. Wilkins, Phys. Rev. Letters 10, 336 (1963); D. J. Scalapino, J. R. Schrieffer, and J. W. Wilkins, Phys. Rev. 148, 263 (1966).
[8]R. C. Dynes, J. P. Carbotte, D. W. Taylor, and C. K. Campbell, Phys. Rev. 178, 713 (1969).
[9]W. L. McMillan and J. M. Rowell, Phys. Rev. Letters 14, 108 (1965).
[10]W. L. McMillan and J. M. Rowell, in *Superconductivity*, edited by R. D. Parks (Dekker, New York, 1969), Chap. 11.
[11]D. J. Scalapino, in *Superconductivity*, edited by R. D. Parks (Dekker, New York, 1969), Chap. 10.
[12]J. M. Rowell and L. Kopf, Phys. Rev. 137, 907 (1965).
[13]J. L. Miles and P. Smith, J. Electrochem. Soc. 110, 1240 (1963).
[14]J. M. Rowell and L. Y. L. Shen, Phys. Rev. Letters 17, 15 (1966); L. Y. L. Shen and J. M. Rowell, Phys. Rev. 165, 566 (1968).
[15]J. Appelbaum, Phys. Rev. Letters 17, 91 (1966); Phys. Rev. 154, 633 (1967); P. W. Anderson, Phys. Rev. Letters 17, 95 (1966).
[16]L. Y. L. Shen (private communication).
[17]L. Y. L. Shen, Phys. Rev. Letters 24, 1104, (1970).
[18]W. L. Feldmann and J. M. Rowell, J. Appl. Phys. 40, 312 (1969).
[19]J. M. Rowell, W. L. McMillan, and W. L. Feldmann, Phys. Rev. 180, 658 (1969).
[20]D. E. Thomas and J. M. Rowell, Rev. Sci. Instr. 36, 1301 (1965).
[21]W. F. Brinkman, R. C. Dynes, and J. M. Rowell, J. Appl. Phys. 41, 1915 (1970).
[22]J. M. Rowell, Bull. Am. Phys. Soc. 12 77 (1967).
[23]W. N. Hubin, Technical Report No. 182, (Department of Physics, University of Illinois, Urbana, Illinois, 1970) (unpublished).
[24]R. J. Pederson, and F. L. Vernon, Jr., Appl. Phys. Letters 10, 29 (1967); I. Giaever, in *Tunneling Phenomena in Solids*, edited by E. Burstein and S. Lundqvist (Plenum, New York, 1969).
[25]P. Morel and P. W. Anderson, Phys. Rev. 125, 1263 (1962).
[26]W. J. Tomasch, Phys. Rev. Letters 15, 672 (1965); 16, 16 (1966).
[27]W. L. McMillan and P. W. Anderson, Phys. Rev. Letters 16, 85 (1966); W. L. McMillan, Phys. Rev. 175, 537 (1968); 175, 559 (1968).
[28]R. C. Dynes, J. P. Carbotte, and E. J. Woll, Jr., Solid State Commun. 6, 101 (1968).
[29]M. J. P. Musgrave, Proc. Roy. Soc. (London) 272, 503 (1963).
[30]R. E. DeWames and G. W. Lehman, Phys. Rev. 135, A170 (1964), and references therein.
[31]W. P. Mason and H. E. Bömmel, J. Acoust. Soc. Am. 28, 930 (1956).
[32]J. A. Rayne and B. S. Chandrasekhar, Phys. Rev. 120, 1658 (1960).
[33]R. E. Schmunk and W. R. Gavin, Phys. Rev. Letters 14, 44 (1965).
[34]J. M. Rowe, B. N. Brockhouse, and E. C. Svensson, Phys. Rev. Letters 14, 554 (1965).
[35]D. Long Price, Proc. Roy. Soc. (London) 300, 25 (1967).
[36]J. M. Rowe, Phys. Rev. 163, 547 (1967).
[37]B. A. Kotov, N. M. Okuneva, and E. L. Plachenova, Fiz. Tverd. Tela 10, 513 (1968) [Sov. Phys. Solid State 10, 402 (1968)].
[38]B. N. Brockhouse, T. Arase, C. Caglioti, K. R. Rao, and A. D. B. Woods, Phys. Rev. 128, 1099 (1962).
[39]G. Gilat, Solid State Commun. 3, 101 (1965).
[40]R. Stedman, L. Almqvist, G. Nilsson, and G. Raunio, Phys. Rev. 162, 545 (1967); 163, 567 (1967); R. Stedman, L. Almqvist, and G. Nilsson, *ibid.* 162, 549 (1967).
[41]J. M. Rowell, W. L. McMillan, and W. L. Feldmann, Phys. Rev. 178, 897 (1969).
[42]D. Long Price (private communication).
[43]D. J. Page, Proc. Phys. Soc. (London) 91, 76 (1967).
[44]M. H. Bredov, B. A. Kotov, N. M. Okuneva, U. S. Oskotskii, and A. L. Shakh-Budagov, Fiz. Tverd. Tela 9, 287 (1967) [Sov. Phys. Solid State 9, 214 (1967)]; B. A. Kotov, N. M. Okuneva, and A. L. Shakh-Budagov, *ibid.* 9, 2553 (1967) [9, 2011 (1968)].
[45]A. P. Roy and B. N. Brockhouse, Can. J. Phys. 48, 1781 (1970).